

**This un-edited manuscript has been accepted for publication in Biophysical Journal and is freely available on BioFast at <http://www.biophysj.org>. The final copyedited version of the paper may be found at <http://www.biophysj.org>.**

**Site-directed fluorescence labeling of a membrane protein with BADAN:  
Probing protein topology and local environment**

Rob B.M. Koehorst, Ruud B. Spruijt and Marcus A. Hemminga\*

Laboratory of Biophysics, Wageningen University,  
Dreijenlaan 3, 6703 HA Wageningen, The Netherlands

Key words: membrane-embedded M13 coat protein; site-specific cysteine mutants;  
fluorescence Stokes shift; hydration level; local polarity; internal label dynamics

Running title: Membrane protein fluorescence labeling

\*Corresponding author: Marcus A. Hemminga  
Laboratory of Biophysics, Wageningen University  
P.O. Box 8128, 6700 ET Wageningen, The Netherlands  
Office: Dreijenlaan 3, 6703 HA Wageningen, The Netherlands  
E-mail: [marcus.hemminga@wur.nl](mailto:marcus.hemminga@wur.nl)  
Telephone: +31-317-482044; Fax: +31-317-482725  
Web site: <http://ntmf.mf.wau.nl/hemminga/>

## Abbreviations used

14:1PC	1,2-Dimyristoleoyl- <i>sn</i> -glycero-3-phosphocholine
16:1PC	1,2-Dipalmitoleoyl- <i>sn</i> -glycero-3-phosphocholine
18:1PC	1,2-Dioleoyl- <i>sn</i> -glycero-3-phosphocholine
18:1PG	1,2-Dioleoyl- <i>sn</i> -glycero-3-[phospho- <i>rac</i> -(1-glycerol)]
20:1PC	1,2-Dieicosenoyl- <i>sn</i> -glycero-3-phosphocholine
AEDANS	N-(acetylaminoethyl)-5-naphthylamine-1-sulfonic acid
Aladan	Artificial fluorescent amino acid
BADAN	6-Bromo-acetyl-2-dimethylamino-naphthalene
HICT <sub>i</sub>	Hydrogen-bonded intramolecular charge transfer state in an immobilized environment
HICT <sub>m</sub>	Hydrogen-bonded intramolecular charge transfer state in a mobile environment or with local mobility
ICT	Intramolecular charge transfer state
LAURDAN	6-Lauroyl-2-(dimethylamino)naphthalene
PICT	Planar intramolecular charge transfer state
PRODAN	6-Propionyl-2-(dimethylamino)naphthalene
TICT	Twisted intramolecular charge transfer state

## **ABSTRACT**

We present a new and simple method based on site-directed fluorescence labeling using the BADAN label that allows to examine protein-lipid interactions in great detail. We apply this approach to a membrane-embedded mainly  $\alpha$ -helical reference protein, the M13 major coat protein, of which in a high-throughput approach 40 site-specific cysteine mutants were prepared of the 50-residues long protein. The steady-state fluorescence spectra are analyzed using a three-component spectral model that enables to separate Stokes shift contributions from water and internal label dynamics, and protein topology. It is found that most of the fluorescence originates from BADAN labels that are hydrogen bonded to water molecules even within the hydrophobic core of the membrane. Our spectral decomposition method reveals the embedment and topology of the labeled protein in the membrane bilayer under various conditions of headgroup charge and lipid chain length, as well as key characteristics of the membrane, such a hydration level and local polarity, given by the local dielectric constant.

## INTRODUCTION

In our previous work on the development of site-directed fluorescent methods to determine the structure of membrane proteins, we have been using AEDANS as a label. For these studies the M13 major coat protein was selected as a reference protein, because its membrane-bound properties have been described in several biophysical studies (for a review, see (1)). Moreover, under the experimental conditions used for the fluorescence experiments, our findings are not complicated by protein-protein interactions (2) and environmental stress (3). From these studies it turns out that the coat protein is a single membrane spanning almost straight  $\alpha$ -helical protein (3-5) that does not differ much from the structure in the intact phage (6). AEDANS has several physicochemical properties that make it a useful label for such investigations: (i) the fluorescent spectrum is a simple line shape of which the position is sensitive to the environmental polarity (i.e., it is an environmental probe) (7-10); (ii) the AEDANS linker is sufficiently long and flexible to enable the probe to sense the global environment and not local molecular effects; (iii) the linker flexibility enables accurate FRET (Förster (or fluorescence) resonance energy transfer) experiments to be carried out on the donor-acceptor pair Trp-AEDANS using an averaged orientation factor  $\kappa^2 = 2/3$  (3-5,11). From the environmental properties of the AEDANS label, also the membrane embedment was found, resulting in a slightly tilted protein topology (10).

The BADAN label (see Fig. 1) is a good alternative for AEDANS. Since it has a shorter linker, its fluorescence spectra could reflect more local molecular details. In this respect BADAN resembles Aladan, a synthetic amino acid, which upon incorporating into a protein has a BADAN-like chromophore at a short distance to the protein backbone (12,13). Therefore, it may be a more accurate monitor for the direct environment of the labeled site. From a photophysical point of view, BADAN is similar to the well-known polarity probes PRODAN and LAURDAN that have been used in several membrane studies. Both probes demonstrate a so-called 'dual fluorescence' behavior that is explained by the presence of at least two excited states of which one is denoted as a locally excited or Franck Condon state and the other is denoted as an intramolecular charge transfer (ICT) state (14-19). In general the solvent dependent red shift of the fluorescence of these labels is, at least partly, ascribed to relaxation of the polar ICT state by reorientation of solvent dipoles. However, in several papers, both of experimental and theoretical nature, the involvement of planar as well as twisted ICT states (PICT and TICT, respectively) was discussed (13,17,20,21). Twisting in the excited state (i.e., rotation or wobbling of the propanoyl moiety with respect to the aromatic ring, see arrow in Fig. 1) is thought to be the most probable mechanism for internal label dynamics (17,21).

From studies of PRODAN and LAURDAN in lipid bilayer systems it is generally accepted that the solvent contribution to the observed shift of the fluorescence spectrum concerns the relaxation of their relatively polar excited state by surrounding water dipoles (16,19,22-27). Thus by using the BADAN label in site-directed studies of membrane-proteins, it could be expected that it will provide more physicochemical details about the protein-lipid-water system as compared to the AEDANS label.

In this paper we present steady-state fluorescence data of site-directed BADAN-labeled M13 coat protein mutants reconstituted in lipid bilayers under various

conditions of headgroup charge and lipid chain length. Analysis of the fluorescent data reveals the embedment and topology of the labeled protein in the membrane bilayer under various conditions of headgroup charge and lipid chain length, as well as key characteristics of the membrane, such a hydration level and local polarity.

## EXPERIMENTAL

### *Sample preparation*

In a high-throughput approach a total of 40 site-specific cysteine mutants of M13 major coat protein were prepared, purified and labeled with 6-bromoacetyl-2-dimethylaminonaphthalene (BADAN; Invitrogen, Molecular Probes, Carlsbad, CA) similar as described previously for labeling with N-(iodoacetylaminoethyl)-5-naphthylamine-1-sulfonic acid (IAEDANS) (8). These mutants cover 80% of the total number of amino acid residues in the primary sequence of the 50-residues long protein. BADAN-labeled M13 coat protein mutants were reconstituted into phospholipid bilayers as reported earlier (28).

The phospholipids 1,2-dimyristoleoyl-*sn*-glycero-3-phosphocholine (14:1PC), 1,2-dipalmitoleoyl-*sn*-glycero-3-phosphocholine (16:1PC), 1,2-dioleoyl-*sn*-glycero-3-phosphocholine (18:1PC), 1,2-dieicosenoyl-*sn*-glycero-3-phosphocholine (20:1PC), were purchased from Avanti Polar Lipids (Alabaster, AL) and 1,2-dioleoyl-*sn*-glycero-3-[phospho-*rac*-(1-glycerol)] (18:1PG) was purchased from Sigma (St. Louis, MO). Apart from the pure phospholipid bilayer systems, a mixed bilayer system was prepared consisting of 18:1PC and 18:1PG in a 4:1 molar ratio, which will be denoted as 18:1PC/18:1PG. Highly diluted phospholipid samples were prepared with a mutant protein concentration of ~1  $\mu$ M. The lipid to protein ratio of all samples was ~1500.

### *Fluorescence measurements*

Fluorescence spectra of the BADAN-labeled mutants in lipid bilayer solutions were recorded using excitation light of 390 nm and an emission detection from 400 to 600 nm, with a 2-nm band pass in both excitation and detection light paths on a Fluorolog 3.22 (Jobin Yvon-Spex, Edison, NJ). Red-edge excitation effects were studied by varying the excitation wavelength between 345 and 405 nm. Steady-state fluorescence anisotropy spectra were recorded using slit widths corresponding to a 5-nm band pass. Analysis of the steady-state spectra was performed using the program IGOR Pro 3.13 (WaveMetrics, Lake Oswego, OR). All experiments were carried out at room temperature (~20 °C).

The unpolarized fluorescence spectra were corrected for the wavelength-dependent sensitivity of the detection system, and were digitally corrected for background signals by subtracting the spectrum of a wild-type protein containing sample having approximately the same protein concentration and lipid to protein ratio. The fluorescence anisotropy,  $r(\lambda)$ , was calculated directly from the uncorrected, polarized fluorescence,  $I(\lambda)$ , as follows:

$$r(\lambda) = \frac{I(\lambda)_{VV} - G(\lambda)I(\lambda)_{VH}}{I(\lambda)_{VV} + 2G(\lambda)I(\lambda)_{VH}}, \quad G(\lambda) = \frac{I(\lambda)_{HV}}{I(\lambda)_{HH}}, \quad (1)$$

where the subscripts refer to the horizontal or vertical settings of the excitation and emission polarizers, respectively.  $G(\lambda)$  compensates for the wavelength-dependent, polarizing effects of the instrument.

## RESULTS AND DISCUSSION

### *Fluorescence anisotropy*

To acquire the steady-state fluorescence anisotropy, a selection of BADAN-labeled M13 coat protein mutants covering the entire primary amino acid sequence in 18:1PC/18:1PG bilayers was studied by exciting the BADAN label around its absorption maximum (385 nm). This resulted in values for the fluorescence anisotropy  $r$  at the fluorescence maximum ranging from  $\sim 0.30$  for mutant positions in the transmembrane protein region to  $\sim 0.25$  for positions in the N-terminal region. The anisotropy values are relatively close to the fundamental anisotropy of a related fluorophore LAURDAN, which are around 0.35 in a vitrified solvent (15,21). Similar high anisotropy values were also reported for Aladan-containing globular proteins (13).

The values for the fluorescence anisotropy  $r$  found for our protein-lipid system are high as compared to what we measure for BADAN in methanol ( $r = 0.01$ ). This indicates that the motion of the BADAN label attached to the labeled protein is restricted. As is shown in Fig. 1, the excitation dipole is parallel to the chain that links the label and protein together (16,29). It is reasonable to assume that the emission dipole has the same orientation. Thus local dynamics (e.g., rotation around the linker axis) may occur without observing a loss of polarization. The fact that close to both termini (positions 3 and 47) also a relatively high anisotropy value is obtained ( $\sim 0.25$ ), suggests that the wobbling motion of the label is restricted throughout the entire protein. For example, a dynamic random coil at both termini would have reduced the anisotropy values considerably. Therefore, the anisotropy data are consistent with our previous finding that the coat protein comprises an almost straight  $\alpha$ -helix (3,11) with an unstructured, non-dynamical N-terminal domain from amino acid residues 1-9 (4,5,30), because in such a conformation one indeed expects the label to show restricted flexibility.

### *Fitting of fluorescence spectra*

In contrast to the fluorescence spectra of membrane-embedded AEDANS-labeled M13 coat protein mutants that consist of a single Gaussian line shape (9,10), the fluorescence spectra of BADAN-labeled M13 coat protein mutants are complex line shapes. This is related to differences in the time scale of the excited state processes as compared to the fluorescence life time, which is shorter for BADAN ( $\leq 5$  ns) than for AEDANS (10 to 20 ns) (31). As a consequence the distribution of fluorescent BADAN species is heterogeneous. The fluorescence spectra of membrane-embedded BADAN-labeled M13 coat protein mutants therefore show variations in position, shape and width resulting from these phenomena. Because several parameters influence the final energy of the excited states, the wavelength of maximum fluorescence is not a useful parameter for the environmental polarity, as is the case for the AEDANS label (7,9,10).

In all cases it turned out that the fluorescence spectra of BADAN-labeled M13 coat protein mutants could be decomposed into three Gaussian line shapes, each characterized by a position ( $P$ ), intensity ( $I$ ) and width ( $W$ ). In the course of this fitting analysis, it was found that the position of two components could be fixed at 23000 and 22000  $\text{cm}^{-1}$ , respectively, which considerably simplified the spectral decomposition. Typical fitting examples are shown in Fig. 2 for the BADAN label positioned close to the bulk water phase (G3C), in the N-terminal domain located in the phospholipid headgroup region (F11C) and the transmembrane domain embedded within the hydrophobic core region of the bilayer (G38C). High-quality fits were obtained, as was judged from the corresponding residual plots in Fig. 2. All other mutants showed fits of similar quality, demonstrating that the spectral decomposition model works fine for all cases studied.

A two or three-component decomposition has been carried out in previous analyses of the fluorescence spectra of a similar fluorophore LAURDAN in biological membranes (32), gel and liquid crystal-phase lipid bilayers (33), and reversed micelles (21). Our spectral decomposition can be related to the proposed energy level scheme of BADAN illustrated in Fig. 3, which schematically shows the heterogeneity of the ground state of BADAN leading to a spectral heterogeneity. The ground state heterogeneity results from differences in hydrogen-bonding capacity of BADAN (see Fig. 1) in polar and apolar environments that subsequently will affect the various excited states.

It has been shown in the literature for PRODAN and LAURDAN, which are structural equivalent to BADAN, that hydrogen bonding results in a lowering of the intramolecular charge transfer (ICT) state to a hydrogen-bonded intramolecular charge transfer (HICT) state (14,15,18,22). By this hydrogen bonding it is believed that in the excited state the negative charge on the carbonyl moiety, which belongs to the electron acceptor part of the BADAN molecule, is stabilized. It should be noted that in the energy level scheme in Fig. 3 we exclude the so-called locally excited (Franck-Condon) state, because it can be assumed that the charge transfer process itself is very fast (15,21).

In connection with the fluorescence spectrum of LAURDAN in low-water gel-phase lipid systems with a maximum around 435 nm ( $\sim 23000 \text{ cm}^{-1}$ ) (22,23,33), we assign the fluorescence component at this position to a non hydrogen-bonded ICT species (Fig. 3). We are allowed to fix its position, because in the absence of hydrogen-bonding water it can be assumed that the ICT state is not subjected to solvent relaxation by water molecules (for simplicity we neglect possible PICT to TICT conversions for the ICT state). In an aqueous environment the BADAN label will be primarily hydrogen bonded. Therefore the contribution of the ICT state in the decomposition is small, as can be seen for BADAN positions close to the bulk water phase (G3C, Fig. 2A) and in the headgroup region (F11C, Fig. 2B).

For LAURDAN in highly viscous ethanol at low temperature ( $-110 \text{ }^\circ\text{C}$ ) a fluorescence spectrum with a maximum around 450 nm is found (15). We may assume that this fluorescence originates from a HICT state, and that solvent relaxation is very slow in this system (15). Based on this observation, it is reasonable to propose that BADAN will show a similar state in lipid systems, in case it is surrounded by

immobilized water molecules. Indeed, from fitting our fluorescence spectra without fixing the position of the fluorescence components (results not shown), the position of one component was consistently found at  $\sim 455$  nm ( $22000 \pm 200$   $\text{cm}^{-1}$ ). Therefore, we decided to fix the position of this component for all spectral decompositions at  $22000$   $\text{cm}^{-1}$ . Since it represents BADAN in an immobilized hydrogen-bonding environment, it will be denoted by  $\text{HICT}_i$  (Fig. 3). A similar fluorescence component is also found for LAURDAN in relatively highly ordered gel-phase lipid bilayers (33) and for Aladan buried in a globular protein core (13).

It is also reported in the literature that upon increasing the temperature of solutions of LAURDAN in ethanol from  $-110$  to  $20$   $^{\circ}\text{C}$ , the fluorescence spectrum gradually evolves into one with its maximum around  $490$  nm (15). Clearly the fluorescence properties of this label change with increasing mobility of its environment. A similar fluorescence component is found for LAURDAN in liquid crystalline-phase lipid bilayers (33). It should be noted, however, that from their data the authors of that paper were not able to discriminate between contributions of internal label dynamics and solvent relaxation. For BADAN-labeled M13 coat protein in a heterogeneous lipid-water environment with free water molecules in the bulk phase and bound water in the phospholipid headgroup region of the lipids, one may also expect fluorescence contributions from hydrogen-bonded species in both a mobile and (partly) immobilized environment, respectively. Therefore in a first approximation, we will describe the spectral contribution of hydrogen-bonded BADAN by two fluorescence contributions, one representing the immobile state ( $\text{HICT}_i$ ) and one for the mobile state ( $\text{HICT}_m$ ). Apart from internal label dynamics, solvent relaxation, i.e., reorientation of the dipoles of the water molecules, will lower the energy of the initial excited state of hydrogen-bonded BADAN labels, if the rotational correlation time of the water molecules is much shorter than the lifetime of the excited state (about  $5$  ns). This lowering effect is strongly dependent on the physicochemical state of the BADAN environment, so that the final energy of the  $\text{HICT}_m$  state and related wavelength of emission (i.e., fluorescence Stokes shift) varies with the local polarity as described by the Lippert equation (34).

Interestingly, for BADAN positions within the hydrophobic core region of the phospholipid bilayer basically a similar three component decomposition is found as for positions outside the bilayer. The occurrence of the fluorescence components at  $23000$  and  $22000$   $\text{cm}^{-1}$  supports the idea that in an apolar environment also the ICT and  $\text{HICT}_i$  states are present. As may be expected, the contribution of the non hydrogen-bonded ICT state has increased with respect to BADAN positions in an aqueous environment (G38C, Fig. 2C). However, the presence of the hydrogen-bonded  $\text{HICT}_i$  state is surprising and suggests that even within the apolar hydrophobic core region of the membrane the BADAN labels are water bonded, probably in a 1:1 complex as shown in Fig. 1. A large binding constant for a 1:1 complex of LAURDAN and ethanol in cyclohexane was recently shown (14). In this case, the third component with variable wavenumber cannot arise from a lowering of the energy of the  $\text{HICT}_i$  state by mobile water molecules. Furthermore, the mobile acyl chains of the phospholipids cannot cause a solvent relaxation effect on the charge-transfer excited state, because their dipole moment is too small. Therefore, we assign the lowering effect of the  $\text{HICT}_i$  state in the hydrophobic core region to internal label dynamics by twisting of the BADAN molecule in the excited state (i.e., rotation or wobbling of the propanoyl moiety with respect to the aromatic ring, see arrow in Fig.



1). In this case, the final energy of the HICT<sub>m</sub> state will depend on the internal label dynamics of the BADAN molecule attached to the protein.

In the case of water-exposed BADAN labels, it may be expected that internal label dynamics of the molecule may also lower the energy of the HICT<sub>i</sub> state. This processes takes place simultaneously with solvent relaxation by water molecules and in our present steady-state approach we are unable to discriminate between these processes.

In summary, the fluorescence spectra of membrane-embedded BADAN-labeled M13 coat protein mutants are decomposed into three fluorescence components, representing the fluorescence of: 1) non hydrogen-bonded BADAN; 2) hydrogen-bonded BADAN in an immobile environment; and 3) hydrogen-bonded BADAN either having an internal label dynamics in a mobile aqueous environment for label positions outside the hydrophobic core of the lipid bilayer, or with only internal label dynamics for label positions inside the core. Our spectral decomposition enables us to study the effect of lipid headgroup charge and lipid chain length on three key BADAN fluorescence parameters:

- $f_{HB}$ : total spectral fraction originating from hydrogen-bonded BADAN labels (sum of contribution of HICT<sub>i</sub> and HICT<sub>m</sub>);
- $f_m$ : spectral fraction originating from mobile state hydrogen-bonded BADAN labels (contribution of HICT<sub>m</sub>);
- $P_m$ : wavenumber position of the mobile state fluorescence component (HICT<sub>m</sub>), which describes the fluorescence of the final relaxed state and is affected by internal dynamics of the label in the excited state and local polarity effects.

The fractions of the spectral components are calculated by taking the product of the corresponding intensity  $I$  and width  $W$  relative to the total. From the fit analyses it is found that the standard deviation of the parameters  $f_{HB}$  and  $f_m$  for BADAN in the N and C-terminal protein domain is about 0.01. In the transmembrane protein domain the standard deviation is somewhat larger, i.e., 0.05. However, the standard deviation of  $P_m$  strongly depends on the spectral fraction  $f_m$ . For values of  $f_m \sim 0.9$  the standard deviation in  $P_m$  is 10 cm<sup>-1</sup>. For  $f_m$  values of 0.5 and 0.2 this is 100 and 500 cm<sup>-1</sup>, respectively.

To confirm the spectral decomposition approach, red-edge excitation experiments were carried out for a selection of BADAN-labeled M13 coat protein mutants covering the entire primary amino acid sequence. For most mutants changing the excitation wavelength from 345 to 405 nm resulted in a small red shift of  $P_m$ , and increase of  $f_{HB}$  and  $f_m$ . Obviously, by optical selection of BADAN labels having an environment more favorable for relaxation of their polar excited state, the probability of exciting hydrogen-bonded species increases. Consequently the spectral contribution of the solvent-relaxed mobile state increases.

### ***Effect of label position***

The effect of label position is shown in Figs. 4A - C, where we plotted the BADAN fluorescence parameters ( $f_{HB}$ ,  $f_m$  and  $P_m$ ) for all 40 membrane-embedded BADAN-

labeled M13 coat protein mutants in 18:1PC bilayers. From these plots one can note that around amino acid positions 25 and 40 the BADAN fluorescence parameters change dramatically. This agrees with earlier studies, in which it was shown that the transmembrane  $\alpha$ -helical domain of the protein runs approximately from residue 21 to 45 (1). Several factors determine the plots in Figs. 4A - C. Some of them are related to the structure and membrane-embedding of the M13 coat protein: tilt, orientation and depth of insertion. Others affect the photophysical state of the BADAN label: local polarity, mobility of environment, internal dynamics of the label, and hydrogen-bonding capacity. All together these factors give rise to irregular oscillations of the parameters in Fig. 4A - C. To disentangle the various effects, we assume the protein to be a perfect  $\alpha$ -helix (3-5) and calculate the distance to a reference position at the center of the bilayer, using the known tilt angle, protein orientation and depth of insertion (10). The center of the BADAN label is taken 7 Å normal to the helical axis, and its position at the virtual amino acid residue number 32.6 (i.e., helical side exactly holding position 29 and exactly opposite to position 38) was taken as the reference position at the center of the bilayer (10). This results in the plots in Figs. 4D - F, which express the BADAN fluorescence parameters now as a function of the distance to the center of the bilayer. In these plots primarily the photophysical parameters of the BADAN label will play a role.

As can be seen in Fig. 4D, at all label positions BADAN is fully hydrogen-bonded, except for positions in the centre of the hydrophobic core of the bilayer, where the spectral fraction of hydrogen-bonded BADAN ( $f_{HB}$ ) is slightly decreased (by about 20%). This decrease is in agreement with the low water concentration in the bilayer interior as found from molecular dynamics simulations (35,36) and in the structure of a fluid 18:1PC bilayer determined by the joint refinement of X-ray and neutron diffraction data (37). As discussed before, it can thus be assumed that in most cases the BADAN labels are water bonded (Fig. 1).

Also the spectral fraction originating from mobile state hydrogen-bonded BADAN labels ( $f_m$ ) is close to 1 for all positions in the water phase and phospholipid headgroup region, but drops to about 0.5 in the hydrophobic core of the bilayer (see the trend line in Fig. 4E). However, label positions 29, 34 and 38 show much lower values. Clearly for label positions outside the hydrophobic core of the lipid bilayer, the BADAN label is sensing mainly a mobile environment, e.g., both the internal label dynamics and water mobility are relatively high. On going to the hydrophobic bilayer interior the local environment of the BADAN label becomes more rigid, and only for about 50% of the BADAN labels internal label dynamics is sufficient to become the relaxation mechanism of the excited HICT state. Internal label dynamics as the origin of the relaxation of the excited state (from about 22000 to 20500  $\text{cm}^{-1}$ ) is confirmed by our observation that increasing the temperature has no effect on  $P_m$  at position 29 in the core, but increases  $f_m$  from 0.38 to 0.61 (data not shown).

The strongly reduced values for label positions 29, 34 and 38 (also position 32 falls in this group) indicate a reduction of the number of labels with internal label dynamics. It is interesting to note that for the tilted membrane-embedded protein, positions 29 and 38 exactly face the tilt (e.g., 29 on one side and 38 opposite to that side). In addition, in an  $\alpha$ -helical protein model, position 32 is close to 29 and position 34 is close to 38. Consequently, all these BADAN labels are placed “above” or “below” the protein, directly facing the termini of the acyl chains of the phospholipids. These

positions can be expected to sense a higher local lipid ordering and reduced lipid mobility as compared to positions at the other sides of the protein helix. This ordering effect will reduce the internal label dynamics and consequently lead to a reduced mobile BADAN fraction. This result agrees well with recent findings from a site-directed spin labeling ESR study of the same protein-lipid systems that around the above mentioned positions in the center of the transmembrane domain the so-called normalized free rotational space of the spin label is reduced (30). Especially amino acid positions 29 and 34 show strongly reduced values for the normalized free rotational space, which is in excellent agreement with the BADAN data. This finding shows that acyl chains are exerting forces on tilted membrane-bound proteins that can be monitored by measuring the fluorescent properties of BADAN labels.

The wavenumber position of the mobile state fluorescence component ( $P_m$ ) is shown in Fig. 4F. Since in the data in Figs. 4D - F we have eliminated the structural effects of the protein-lipid system, the remaining dependence of label depth in the bilayer will result from mainly local polarity effects (i.e., the local dielectric constant  $\epsilon$ ) as sensed by the BADAN label. Thus, a low or high value of  $P_m$  corresponds to a polar or an apolar environment, respectively. The trend line through the data shows a profile over the phospholipid bilayer that roughly follows the water penetration in the phospholipid bilayer (37,38), resulting in a concomitant change in local dielectric constant  $\epsilon$ . On top of this profile, deviations are again observed in the hydrophobic core of the lipid bilayer, especially for label positions in the C-terminal part of the transmembrane protein domain. These label positions are close to the three lysine residues (Lys40, Lys43, and Lys44) and two phenylalanine residues (Phe42 and Phe45) that provide a very strong anchoring domain for the C-terminal part of the protein (1). The presence of this anchoring domain could result in a change of local water distribution, or lipid packing.

For simplicity, we have assumed that the M13 coat protein can be described by a full  $\alpha$ -helix. However, from previous work it is known that the amino acid residues 1-9 are unstructured (4,5,30). These amino acid positions are located on the N-terminal hydrophilic anchor that is emerging from the headgroup region into the water phase, given by distances from the bilayer centre  $>30$  Å in Fig. 4F (4). The presence of an unstructured protein domain explains the limited fit to the data in this water-lipid region. The fluorescence maximum for PRODAN in water is around 530 nm ( $18860$   $\text{cm}^{-1}$ ). For position 3 we find a higher value for  $P_m$  of  $19200$   $\text{cm}^{-1}$ . This indicates that even at the N-terminal end of the membrane-embedded protein the BADAN labels are not sensing a bulk water environment, probably arising from the fact that the BADAN label has a short linker to the protein backbone.

In conclusion, the analysis of the BADAN fluorescence parameters ( $f_{\text{HB}}$ ,  $f_m$  and  $P_m$ ) shows that most of the fluorescence originates from BADAN labels that are hydrogen bonded to water molecules even within the hydrophobic core of the membrane. The data are consistent with a tilted membrane-embedded structure of the M13 coat protein and a Gaussian profile for the dielectric constant  $\epsilon$  over the membrane.

### ***Effect of headgroup charge***

The effect of headgroup charge was studied by comparing all 40 BADAN-labeled protein mutants in pure 18:1PC and mixed 18:1PC/18:1PG bilayers (Fig. 5). The

effect of headgroup charge is a small increase of the spectral fraction of hydrogen-bonded BADAN ( $f_{\text{HB}}$ ) (Fig. 5A). In the transmembrane protein domain (i.e., label positions in the core of the membrane) the effect of headgroup charge on the spectral fraction of mobile state hydrogen-bonded BADAN labels ( $f_{\text{m}}$ ) is small (Fig. 5B). However, for label positions in the C and N-terminal domain (label positions 10-24 and 42-50), which are in the headgroup region, a consistent decrease on  $f_{\text{m}}$  is seen upon addition of the negatively charged 18:1PG to pure 18:1PC. This indicates a decrease of mobility of the local environment, which most likely results from an increase in bound water molecules at the negatively charged headgroup region. Water molecules in the headgroup region are motionally restricted by hydrogen bonding with lipid headgroups as is confirmed by the observation that  $P_{\text{m}}$  of mutant A18C decreases upon increasing temperature from 20 to 70 °C (data not shown). This decrease of  $P_{\text{m}}$  indicates an increase of relaxation by water becoming more dynamic at higher temperatures. In contrast, the value of  $P_{\text{m}}$  of mutant G3C is not changing upon increasing temperature, as can be expected, because the N-terminus has earlier been shown to reside in the highly mobile water phase (4). Recent results of molecular dynamics simulations (39) also show that hydrogen bonding to the glycerol group of POPG (1-palmitoyl-2-oleoyl-phosphatidylglycerol) slows down water motion more than the choline group of POPC (1-palmitoyl-2-oleoyl-phosphatidylcholine).

Overall the BADAN fluorescence spectrum is slightly red shifted for mixed 18:1PC/18:1PG as compared to pure 18:1PC. This is reflected by a decrease of  $P_{\text{m}}$  as seen in Fig. 5C for almost all label positions. This decrease indicates an overall increased polarity, which is in agreement with an enhanced hydration level of the membrane resulting from an increased intermolecular spacing of the phospholipid headgroups (23). This enhanced hydration level is also in agreement with the increase of  $f_{\text{HB}}$  in Fig. 5A.

However, in Fig. 5 no shift in the patterns of the BADAN fluorescence parameters is seen, as compared to the length and position of the putative transmembrane domain, indicating that changing the charge of the phospholipid headgroups under the current conditions does not affect the topology and membrane-embedment of the M13 coat protein.

### ***Effect of lipid chain length***

The increase of phospholipid acyl chain length on going from 14:1PC to 20:1PC on the BADAN fluorescence parameters ( $f_{\text{HB}}$ ,  $f_{\text{m}}$  and  $P_{\text{m}}$ ) is shown in Fig. 6 for all 40 membrane-embedded BADAN-labeled protein mutants. It should be noted that under the experimental conditions (room temperature) all bilayer systems are in the liquid crystalline phase, as the gel-to-liquid crystalline phase transition temperature of the thickest 20:1PC is about -5 °C (40). It can be seen that for mutant positions in the N-terminal domain, or at the C-terminal domain (i.e., in the headgroup regions and bulk water),  $f_{\text{HB}}$  and  $f_{\text{m}}$  are close to 1, irrespective of bilayer thickness (Fig. 6A and B). This indicates that the hydrogen bonding capacity of the BADAN label and its internal dynamics in this region of the lipid-water system are not affected by a change in bilayer thickness. This is in agreement with molecular dynamics results showing that the water diffusion coefficient is not affected by bilayer thickness (41).

On the other hand, for label positions in the transmembrane region  $f_{\text{HB}}$  and  $f_{\text{m}}$  decrease upon increasing acyl chain length, the effect being substantial large for  $f_{\text{m}}$ . The relatively small decrease of  $f_{\text{HB}}$  for positions in the centre of the transmembrane region in the bilayer centre upon increasing acyl chain length (Fig. 6A) indicates a reduction of the fraction of hydrogen-bonded BADAN labels in the bilayer. This decrease suggests more apolar character and a reduced water concentration in the hydrophobic core of thick bilayers as compared to thin bilayers, in agreement with a reduced water permeability upon increasing acyl chain length demonstrated by molecular dynamics simulations (41).

The spectral fraction originating from mobile state hydrogen-bonded BADAN labels ( $f_{\text{m}}$ ) in the transmembrane region is affected mainly by the internal label dynamics of the BADAN labels. As discussed above, BADAN label positions that are “above” or “below” the  $\alpha$ -helical transmembrane protein domain, are directly facing the termini of the acyl chains of the phospholipids. Therefore they sense a higher local lipid ordering and reduced lipid mobility as compared to positions at the other sides of the protein helix. This effect becomes stronger when the acyl chains are longer, even though the tilt will reduce in this case (10).

The effect of phospholipid acyl chain length on the wavenumber position of the mobile state fluorescence component ( $P_{\text{m}}$ ) is shown in Fig. 6C. As discussed before,  $P_{\text{m}}$  depends primarily on the local polarity (i.e., the local dielectric constant  $\epsilon$ ) that is sensed by the BADAN label. For all lipid systems there is a sharp increase in  $P_{\text{m}}$  in the N-terminal domain around label position 25. At the C-terminal domain a similar effect is seen between positions 41 to 50. These changes of  $P_{\text{m}}$  reflect the drop in local polarity at positions where the transmembrane protein enters and leaves the apolar hydrophobic core region of the bilayer. It is interesting to note that these positions remain the same, irrespective of the bilayer thickness. This observation indicates that the protein responds to a change in bilayer thickness by a change in tilt angle, thereby keeping the transmembrane domain as much as possible embedded in the bilayer. This conclusion is in agreement with previous work (10).

Upon increasing the phospholipid acyl chain length on going from 14:1PC to 20:1PC, a consistent increase of  $P_{\text{m}}$  is observed for BADAN label positions in the N-terminal domain from 13 to 25 (Fig. 6C). These positions are mainly located in the headgroup region of the phospholipid bilayers. The increase of  $P_{\text{m}}$  indicates that upon increasing the hydrophobic thickness the BADAN label will gradually experience a less polar environment. The same phenomenon may be seen when comparing the data for label positions 41 to 50 in the C-terminal domain at the opposite headgroup region of the bilayer. As discussed for the headgroup charge effects, this indicates a reduced hydration level upon increasing acyl chain length close to the glycerol/acyl chain interface.

In conclusion, we have presented a new and simple method based on site-directed fluorescence labeling using the BADAN label that allows to examine protein-lipid interactions in great detail. By using our three-component spectral model, we are able to separate Stokes shift contributions from water and internal label dynamics, and protein topology. The method can reveal the embedment of the labeled protein in the membrane bilayer, as well as key characteristics of the membrane, such a hydration level and local polarity (i.e., the local dielectric constant  $\epsilon$ ).

## REFERENCES

1. Stopar, D., R. B. Spruijt, and M. A. Hemminga. 2006. Anchoring mechanisms of membrane-associated M13 major coat protein. *Chem. Phys. Lipids* 141:83-93.
2. Fernandes, F., L. M. S. Loura, M. Prieto, R. Koehorst, R. B. Spruijt, and M. A. Hemminga. 2003. Dependence of M13 major coat protein oligomerization and lateral segregation on bilayer composition. *Biophys J* 85:2430-2441.
3. Vos, W. L., R. B. M. Koehorst, R. B. Spruijt, and M. A. Hemminga. 2005. Membrane-bound conformation of M13 major coat protein: A structure validation through FRET-derived constraints. *J Biol Chem* 280:38522-38527.
4. Nazarov, P. V., R. B. M. Koehorst, W. L. Vos, V. V. Apanasovich, and M. A. Hemminga. 2007. FRET study of membrane proteins: Determination of the tilt and orientation of the N-terminal domain of M13 major coat protein. *Biophys J* 92:1296-1305.
5. Vos, W. L., M. Schor, P. V. Nazarov, R. B. M. Koehorst, R. B. Spruijt, and M. A. Hemminga. 2007. Structure of membrane-embedded M13 major coat protein is insensitive to hydrophobic stress. *Biophys J* 93:3541-3547.
6. Marvin, D. A. 1998. Filamentous phage structure, infection and assembly. *Curr Opin Struct Biol* 8:150-158.
7. Spruijt, R. B., C. J. A. M. Wolfs, J. W. G. Verver, and M. A. Hemminga. 1996. Accessibility and environment probing using cysteine residues introduced along the putative transmembrane domain of the major coat protein of bacteriophage M13. *Biochemistry* 35:10383-10391.
8. Spruijt, R. B., A. B. Meijer, C. J. A. M. Wolfs, and M. A. Hemminga. 2000. Localization and rearrangement modulation of the N-terminal arm of the membrane-bound major coat protein of bacteriophage M13. *Biochim Biophys Acta* 1508:311-323.
9. Spruijt, R. B., C. J. A. M. Wolfs, and M. A. Hemminga. 2004. Membrane assembly of M13 major coat protein: Evidence for a structural adaptation in the hinge region and a tilted transmembrane domain. *Biochemistry* 43:13972-13980.
10. Koehorst, R. B. M., R. B. Spruijt, F. J. Vergeldt, and M. A. Hemminga. 2004. Lipid bilayer topology of the transmembrane  $\alpha$ -helix of M13 major coat protein and bilayer polarity profile by site-directed fluorescence spectroscopy. *Biophys J* 87:1445-1455.
11. Nazarov, P. V., R. B. M. Koehorst, W. L. Vos, V. V. Apanasovich, and M. A. Hemminga. 2006. FRET study of membrane proteins: Simulation-based fitting for analysis of membrane protein embedment and association. *Biophys J* 91:454-466.

12. Cohen, B. E., T. B. McAnaney, E. S. Park, Y. N. Jan, S. G. Boxer, and L. Y. Jan. 2002. Probing protein electrostatics with a synthetic fluorescent amino Acid. *Science* 296:1700-1703.
13. Abbyad, P., X. Shi, W. Childs, T. B. McAnaney, B. E. Cohen, and S. G. Boxer. 2007. Measurement of solvation responses at multiple sites in a globular protein. *J. Phys. Chem. B* 111:8269-8276.
14. Józefowicz, M., K. A. Kozyra, J. R. Heldt, and J. Heldt. 2005. Effect of hydrogen bonding on the intramolecular charge transfer fluorescence of 6-dodecanoyl-2-dimethylaminonaphthalene. *Chem. Phys.* 320:45-53.
15. Viard, M., J. Gallay, M. Vincent, O. Meyer, B. Robert, and M. Paternostre. 1997. Laurdan solvatochromism: solvent dielectric relaxation and intramolecular excited-state reaction. *Biophys J* 73:2221-2234.
16. Parasassi, T., E. K. Krasnowska, L. Bagatolli, and E. Gratton. 1998. Laurdan and Prodan as polarity-sensitive fluorescent membrane probes. *J. Fluoresc.* 8:365-373.
17. Lobo, B. C. and C. J. Abelt. 2003. Does PRODAN possess a planar or twisted charge-transfer excited state? Photophysical properties of two PRODAN derivatives. *J. Phys. Chem. A* 107:10938-10943.
18. Samanta, A. and R. W. Fessenden. 2000. Excited state dipole moment of PRODAN as determined from transient dielectric loss measurements. *J. Phys. Chem. A* 104:8972-8975.
19. Jurkiewicz, P., J. Sýkora, A. Olżyńska, J. Humpolícková, and M. Hof. 2005. Solvent relaxation in phospholipid bilayers: principles and recent applications. *J. Fluoresc.* 15:883-894.
20. Parusel, A. B. J., W. Nowak, S. Grimme, and G. Kohler. 1998. Comparative theoretical study on charge-transfer fluorescence probes: 6-propanoyl-2-(N,N-dimethylamino)naphthalene and derivatives. *J. Phys. Chem. A* 102:7149-7156.
21. Vincent, M., B. de Foresta, and J. Gallay. 2005. Nanosecond dynamics of a mimicked membrane-water interface observed by time-resolved Stokes shift of LAURDAN. *Biophys J* 88:4337-4350.
22. Parasassi, T. and E. Gratton. 1995. Membrane lipid domains and dynamics as detected by Laurdan fluorescence. *J. Fluoresc.* 5:59-69.
23. Bagatolli, L. A., E. Gratton, and G. D. Fidelio. 1998. Water dynamics in glycosphingolipid aggregates studied by LAURDAN fluorescence. *Biophys J* 75:331-341.
24. Sýkora, J., P. Kapusta, V. Fidler, and M. Hof. 2002. On what time scale does solvent relaxation in phospholipid bilayers happen? *Langmuir* 18:571-574.

25. Krasnowska, E. K., E. Gratton, and T. Parasassi. 1998. Prodan as a membrane surface fluorescence probe: Partitioning between water and phospholipid phases. *Biophys J* 74:1984-1993.
26. Söderlund, T., J.-M. I. Alakoskela, A. L. Pakkanen, and P. K. J. Kinnunen. 2003. Comparison of the effects of surface tension and osmotic pressure on the interfacial hydration of a fluid phospholipid bilayer. *Biophys J* 85:2333-2341.
27. Zhang, Y.-L., J. A. Frangos, and M. Chachisvilis. 2006. Laurdan fluorescence senses mechanical strain in the lipid bilayer membrane. *Biochem Biophys Res Commun* 347:838-841.
28. Spruijt, R. B., C. J. A. M. Wolfs, and M. A. Hemminga. 1989. Aggregation-related conformational change of the membrane-associated coat protein of bacteriophage M13. *Biochemistry* 28:9158-9165.
29. Celli, A., S. Beretta, and E. Gratton. 2007. Phase fluctuation on the micron-submicron scale in GUVs composed of a binary lipid mixture. *Biophys J* 94:104-116.
30. Stopar, D., J. Strancar, R. B. Spruijt, and M. A. Hemminga. 2006. Motional restrictions of membrane proteins: A site-directed spin labeling study. *Biophys J* 91:3341-3348.
31. Hammarström, P., R. Owenius, L.-G. Mårtensson, U. Carlsson, and M. Lindgren. 2001. High-resolution probing of local conformational changes in proteins by the use of multiple labeling: unfolding and self-assembly of Human Carbonic Anhydrase II monitored by spin, fluorescent, and chemical reactivity probes. *Biophys J* 80:2867-2885.
32. Vanounou, S., D. Pines, E. Pines, A. H. Parola, and I. Fishov. 2002. Coexistence of domains with distinct order and polarity in fluid bacterial membranes. *Photochem Photobiol* 76:1-11.
33. De Vequi-Suplicy, C., C. Benatti, and M. Lamy. 2006. Laurdan in fluid bilayers: position and structural sensitivity. *J. Fluoresc.* 16:431-439.
34. Lakowicz, J. R. 2006. *Principles of fluorescence spectroscopy*, 3rd Ed. Springer, New York.
35. Chiu, S. W., E. Jakobsson, S. Subramaniam, and H. L. Scott. 1999. Combined Monte Carlo and molecular dynamics simulation of fully hydrated dioleoyl and palmitoyl-oleoyl phosphatidylcholine lipid bilayers. *Biophys J* 77:2462-2469.
36. Berkowitz, M. L., D. L. Bostick, and S. Pandit. 2006. Aqueous solutions next to phospholipid membrane surfaces: Insights from simulations. *Chem. Rev.* 106:1527-1539.



37. White, S. H. and W. C. Wimley. 1998. Hydrophobic interactions of peptides with membrane interfaces. *Biochim Biophys Acta* 1376:339-352.
38. Marsh, D. 2002. Membrane water-penetration profiles from spin labels. *Eur Biophys J* 31:559-562.
39. Murzyn, K., W. Zhao, M. Karttunen, M. Kurdziel, and T. Rog. 2006. Dynamics of water at membrane surfaces: effect of headgroup structure. *Biointerphases* 1:98-105.
40. Koynova, R. and M. Caffrey. 1998. Phases and phase transitions of the phosphatidylcholines. *Biochim Biophys Acta* 1376:91-145.
41. Sugii, T., S. Takagi, and Y. Matsumoto. 2005. A molecular-dynamics study of lipid bilayers: Effects of the hydrocarbon chain length on permeability. *J. Chem. Phys.* 123:184714-847148.
42. Ridder, A. N. J. A., W. van de Hoef, J. Stam, A. Kuhn, B. de Kruijff, and J. A. Killian. 2002. Importance of hydrophobic matching for spontaneous insertion of a single-spanning membrane protein. *Biochemistry* 41:4946-4952.

## FIGURE LEGENDS

Figure 1. Structural formula of the fluorescence label BADAN covalently linked to the cysteine sulfur, and hydrogen-bonded to a water molecule via its carbonyl oxygen (schematically indicated by a dashed line). The arrow around the bond between the dimethylamino group and the aromatic ring indicates label dynamics (rotation or wobbling) in the excited state. The large arrow represents the excitation dipole (16,29), with its orientation being parallel to the above mentioned rotation axis.

Figure 2. Gaussian decomposition of fluorescence spectra of BADAN-labeled mutants G3C (A), F11C (B) and G38C (C) in 18:1PC/18:1PG bilayers (large dots) including the fit (solid line). The position of the Gaussian line shapes at  $23000\text{ cm}^{-1}$  (long dashes) and  $22000\text{ cm}^{-1}$  (small dashes) is fixed. The position of the high-wavenumber component (small dots) is fitted. Residual plots are scaled between  $\pm 10\%$  of the spectral intensity.

Figure 3. Schematic energy level diagram of BADAN showing the non hydrogen-bonded ICT state and hydrogen-bonded HICT states in an immobilized environment (HICT<sub>i</sub>) and in a mobile environment (HICT<sub>m</sub>). The energy difference between the latter two results from solvent relaxation (SR) by water molecules, and internal label dynamics (LD). The style of the vectors illustrating the emission corresponds with the style of the fluorescence components in Fig. 2.

Figure 4. BADAN fluorescence parameters  $f_{\text{HB}}$  (A and D),  $f_{\text{m}}$  (B and E), and  $P_{\text{m}}$  (C and F) for 40 different mutants in 18:1PC bilayers vs. label positions (A, B and C) and vs. distance from centre (D, E and F). The transmembrane (TM) protein domain runs from label position 21 to 45 (1). The solid vertical lines represent the full bilayer thickness ( $59.5\text{ \AA}$ ); the dotted vertical lines represent the acyl chain/glycerol backbone interfaces (the hydrophobic thickness is  $29.5\text{ \AA}$ ) (37,42). The solid trend lines are Gaussian fits to the data points, excluding the strongly scattered data points from positions 29, 34, and 38 (E) and positions 38, 41 and 46 (F) (see text).

Figure 5. BADAN fluorescence parameters  $f_{\text{HB}}$  (A),  $f_{\text{m}}$  (B), and  $P_{\text{m}}$  (C) for 40 different mutants (position of labeled cysteine on horizontal axis) as function of the composition of the lipid headgroup region (18:1PC: closed triangles; 18:1PC/18:1PG: open circles). The transmembrane (TM) domain runs from position 21 to 45 (1). Data points for adjacent label positions are connected by a line.

Figure 6. BADAN fluorescence parameters  $f_{\text{HB}}$  (A),  $f_{\text{m}}$  (B), and  $P_{\text{m}}$  (C) for 40 different mutants (position of labeled cysteine on horizontal axis) as function of lipid acyl chain length (14:1PC: solid line; 16:1PC: dotted line; 18:1PC: small dashes; 20:1PC: long dashes). The transmembrane (TM) protein domain for 18:1PC is indicated (see Fig. 5). Data points for adjacent label positions are connected by a line.

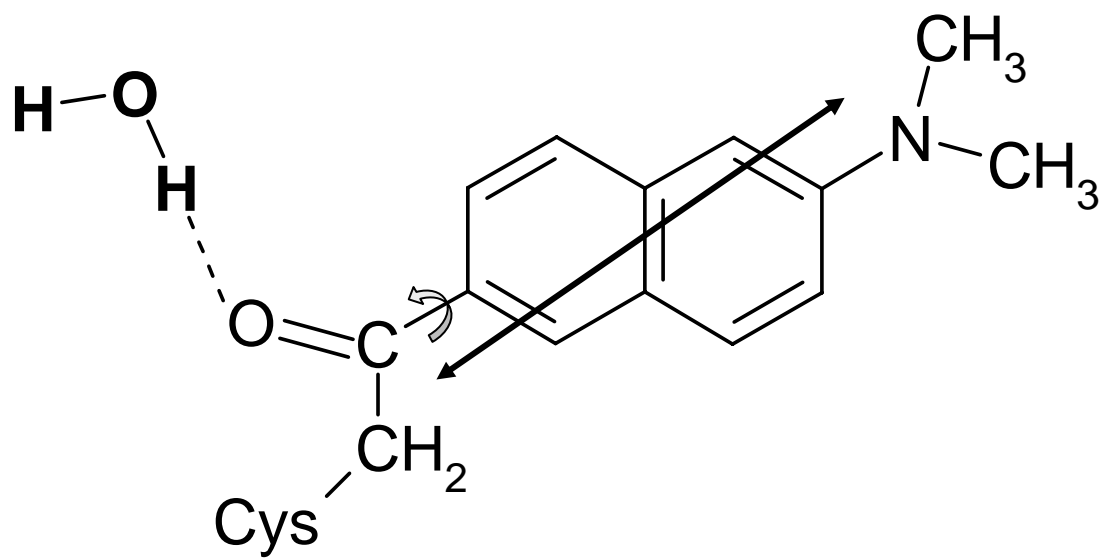


Figure 1

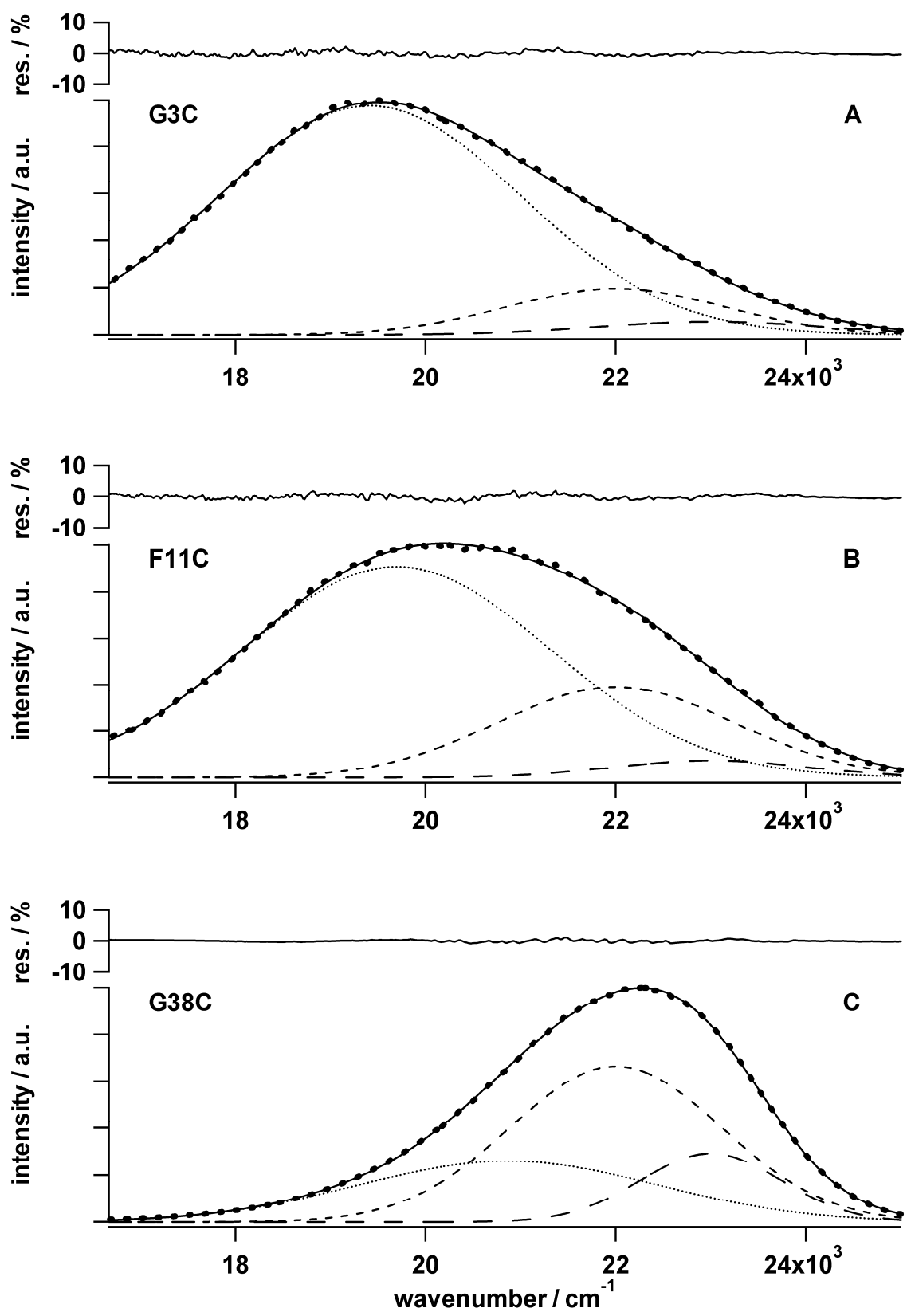


Figure 2

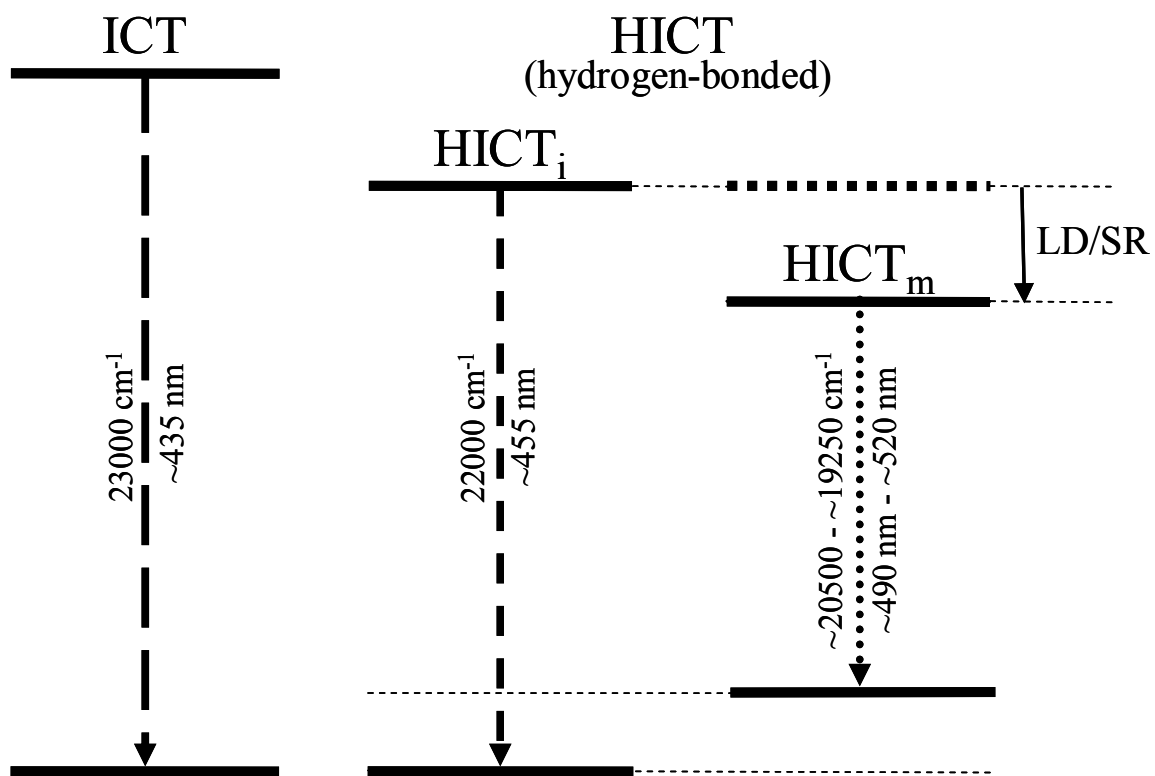


Figure 3

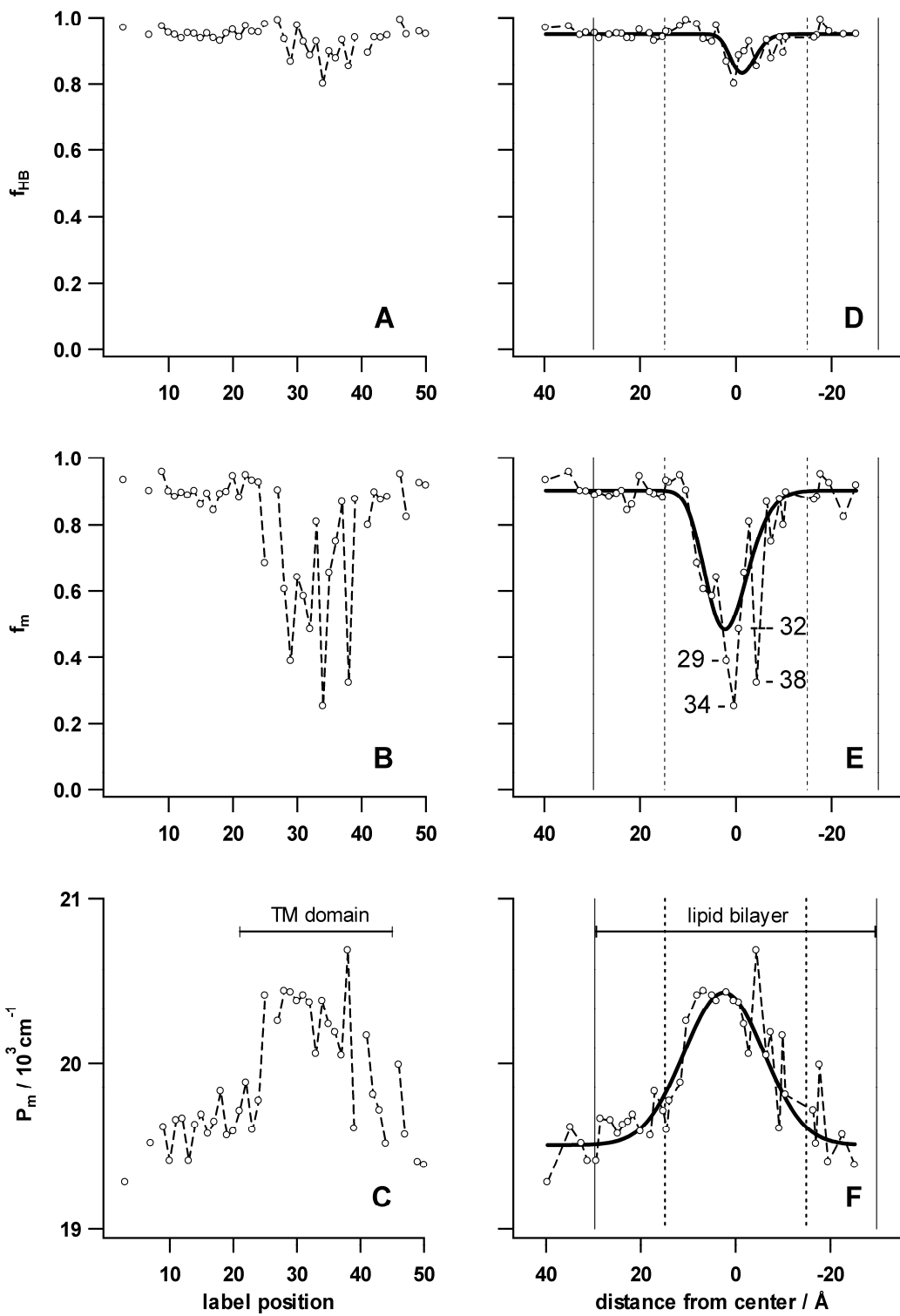


Figure 4

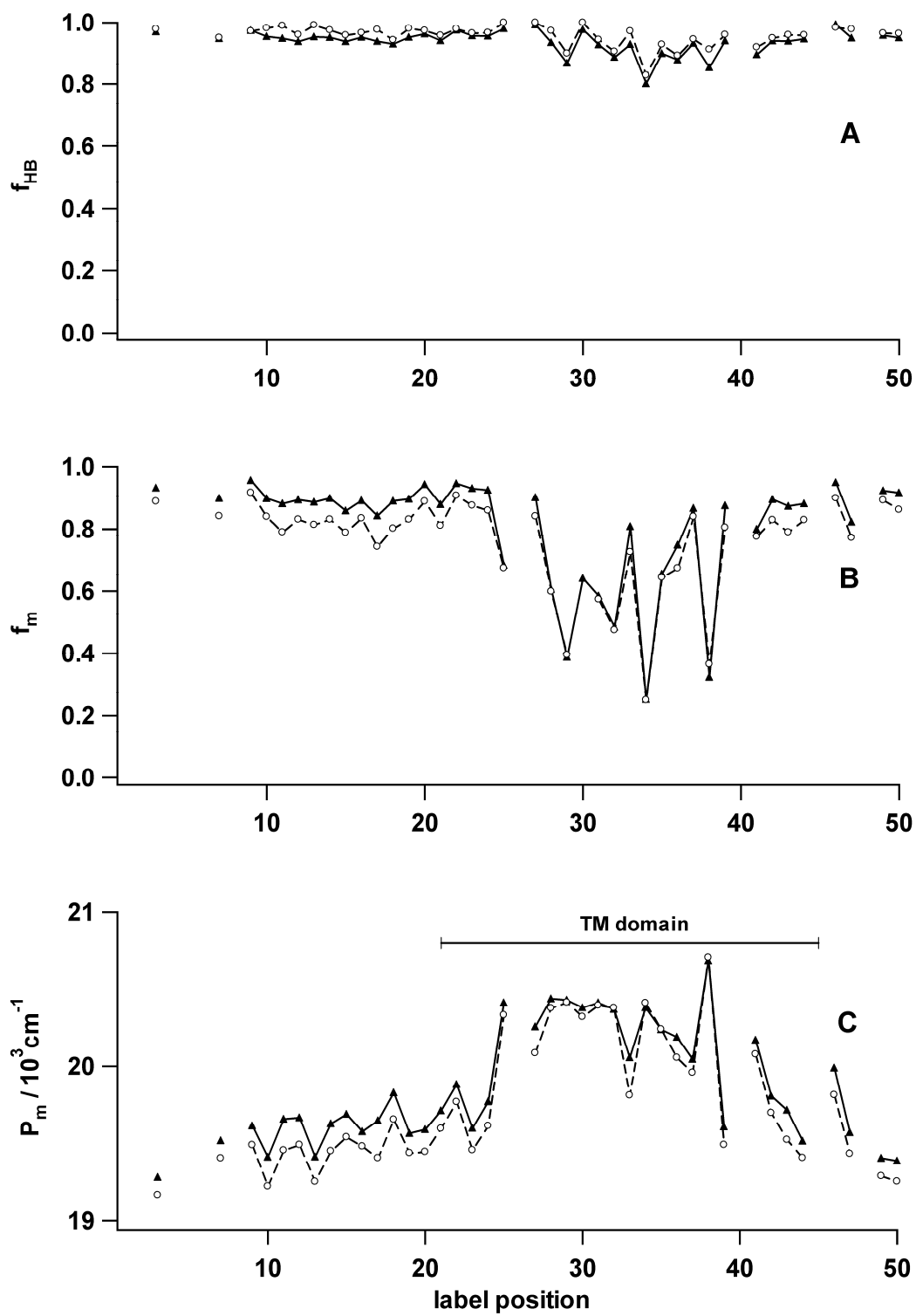


Figure 5

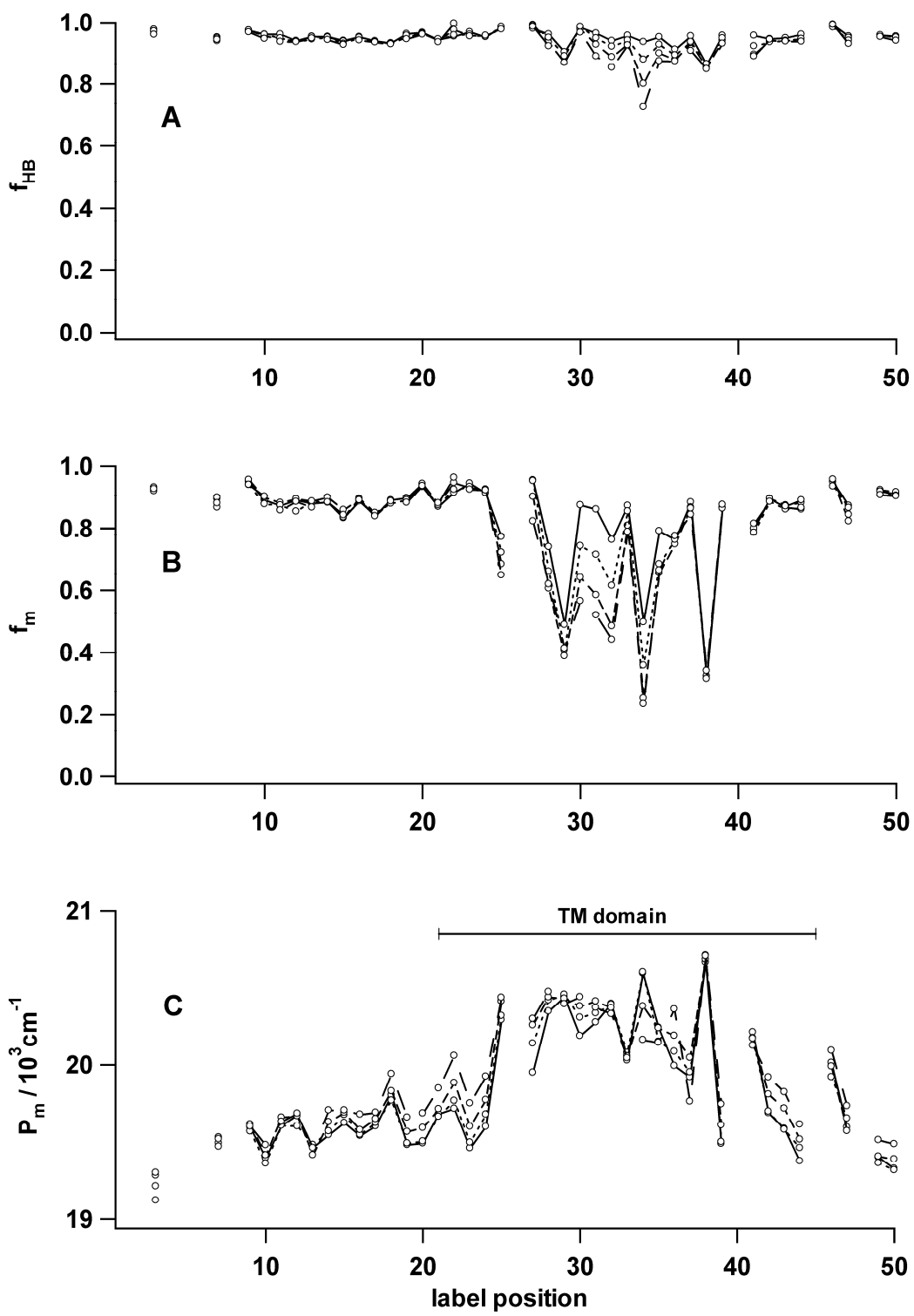


Figure 6